Cost Optimization of a Microgrid Considering Vehicle-To-Grid Technology and Demand Response

Muhammed Ali Beyazıt[1], Akın Taşcıkaraoğlu[1,*], João P. S. Catalão[2]

[1]*Electrical and Electronics Engineering Department, Mugla Sitki Kocman University, Mugla, Turkey*

[2]*Faculty of Engineering of the University of Porto and INESC TEC, Porto 4200-465, Portugal*

** akintascikaraoglu@mu.edu.tr*

Abstract

Demand response (DR) programs can offer various benefits especially in microgrid environments with renewable energy systems (RESs) and energy storage technologies when effectively planned and managed. Accordingly, this study proposes an energy management approach for a neighborhood including residential end-users with photovoltaic (PV) systems, a shared energy storage system (ESS) and an electric vehicle (EV) fleet. The proposed approach presents a novel energy credit mechanism (ECM) for the EV fleet and households separately to exploit the EV batteries and store the excess PV energy in the neighborhood through the shared ESS for later use. End-users gain energy credits before a DR event and use these credits during the peak periods to minimize their total energy cost (TEC), resulted in a decrease in the peak demand. Also, the energy credits gained by the EV fleet are used through the vehicle-to-home (V2H) and vehicle-to-grid (V2G) services with the same objective. In order to conduct a more realistic analysis, a battery degradation cost estimation model is employed and the uncertain behavior of the EV users is considered. The case studies show that the proposed optimization strategy has the capability of considerably reducing the energy costs and peak demand.

Keywords: Demand response, electric vehicles, energy storage systems, microgrid, vehicle-to-grid.

Nomenclature

The nomenclature used throughout the paper is given below.

A. Indices

e	Index of electric vehicles.
h	Index of houses.
t	Index of time periods.

B. Sets

E	Set of all electric vehicles.
H	Set of all houses.
T	Set of all time periods.

C. Parameters

CC	Capital cost of an EV battery.
C_{labor}	Labor cost to replace the battery.
C_e^{deg}	Degradation cost of the battery in \$/kwh for EV e.
$\mathrm{C_{unit}}$	Battery cost in \$/kWh.
DoD	Depth of Discharge.
$E_h^{Crd,0}$	Initial credit of house h.
$E_e^{Crd,EV0}$	Initial credit of EV e.
$E_h^{Crd,max}$	Credit limit of house h.
$LD_{h,t}$	Load demand of house h in time period t.
N	Sufficiently large positive integer.
N_{cycle}	Battery cycle life.
P^{TR}	Power limit of the transformer.
P_{EV}^{CH}	EV charging power limit.
P_{ESS}^{CH}	ESS charging power limit.
P_{ESS}^{DCH}	ESS discharging power limit.
P_{EV}^{DCH}	EV discharging power limit.
$P_{h,t}^{PV}$	PV power produced by house h in time period t.
PV_h^{cap}	Power production capacity for house h.

$PV^{cap,tot}$	Total PV power production capacity in neighborhood.
$SOE^{ESS,0}$	ESS initial energy level.
$SOE^{ESS,max}$	ESS maximum energy level.
$SOE^{ESS,min}$	ESS minimum energy level.
$SOE_e^{EV,0}$	EV initial energy level.
$SOE_e^{EV,cap}$	EV maximum energy level.
$SOE_e^{EV,min}$	EV minimum energy level.
SV	Salvage value of an EV battery.
T_{arr}	Arrival time of EVs.
$T^{DR,end}$	DR event ending time.
$T^{DR,start}$	DR event starting time.
T^{end}	Ending time of the day.
ΔT	A certain time period.
λ_t^{buy}	Energy purchasing price.
λ_t^{sell}	Energy selling price.
η^{CH}	Charging efficiency of the ESS and EVs.
η^{DCH}	Discharging efficiency of the ESS and EVs.

D. Variables

$b_t^1, b_t^2, b_{e,t}^3, b_{h,e,t}^4$	Binary variables (1 or 0 in time period t).
$E_{h,t}^{Crd}$	Energy credit gained by house h in time period t.
$E_{e,t}^{Crd,EV}$	Energy credit gained by EV e in time period t.
$P_{h,t}^{buy,ESS}$	Power provided from the ESS to the house h in time period t.
$P_{e,t}^{buy,EV}$	Power provided from the EV e to the houses in time period t.
$P_{h,t}^{buy,G}$	Power provided from the grid by house h in time period t.
$P_{h,t}^{buy,L}$	Local power provided from the neighborhood to the house h in time period t.
$P_{h,e,t}^{buy,T}$	Total power purchased by house h and EV e in time period t.
$P_t^{ESS,ch}$	ESS charging power in time period t.
$P_t^{ESS,dch}$	ESS discharging power in time period t.
$P_t^{ESS\rightarrow G}$	ESS power provided to the grid in time period t.

$P_t^{ESS\to N}$	ESS power provided to the neighborhood in time period t.
$P_{e,t}^{EV,ch}$	Charging power of EV e in time period t.
$P_{e,t}^{EV,dch}$	Discharging power of EV e in time period t.
$P_{e,t}^{EV\to G}$	The power of EV e transferred to the grid in time period t.
$P_{e,t}^{EV\to N}$	The power of EV e transferred to the neighborhood in time period t.
$P_t^{G\to ESS}$	Total power transferred from grid to ESS in time period t.
$P_{e,t}^{G\to EV}$	Total power transferred from grid to EV e in time period t.
$P_t^{G\to N}$	Total power drawn from grid to the neighborhood in time period t.
$P_t^{G\to TR}$	Total power purchased from grid via transformer in time period t.
$P_t^{N\to ESS}$	Neighborhood surplus power provided to the ESS in time period t.
$P_{e,t}^{N\to EV}$	Neighborhood surplus power delivered to EV e in time period t.
$P_t^{N\to G}$	Total power delivered from neighborhood to the grid in time period t.
$P_{h,t}^{PV,used}$	PV power used by house h to satisfy energy demand in time period t.
$P_{h,t}^{sell,ESS}$	Power provided by house h to the ESS in time period t.
$P_{e,t}^{sell,EV}$	Power provided by houses to the EV e in time period t.
$P_{h,t}^{sell,G}$	Power provided by the house h to the grid in time period t.
$P_{h,t}^{sell,L}$	Power provided by house h to the neighborhood in time period t.
$P_{h,e,t}^{sell,T}$	Total power sold by house h and EV e in time period t.
$P_t^{TR\to G}$	Total power transferred to the grid via transformer in time period t.
SOE_t^{ESS}	Energy level of the ESS in time period t.
$SOE_{e,t}^{EV}$	Energy level the EV e in time period t.
σ	Battery capacity in kWh.

1. Introduction

1.1 Motivation and Relevant Background

Increasing environmental pollution and greenhouse gases forces the policymakers to take regulatory and other structural measures about the zero-emission vehicles and fuel economy standards [1]. As a consequence of policies and in response to technological developments and growing market in the recent years, electric vehicles (EVs) have grown in popularity significantly. The sales of EVs topped 3 million globally and despite the pandemic-related downturn in car sales, the EV registration increased by 41% in 2020 according to the International Energy Agency (IEA) [2].

Implementing a new generation of electric loads with high power and energy values, however, has caused a significant change on the demand side [3]. In order to address the operational challenges caused by these changes in power grids, the incorporation of demand response (DR) programs into power system operation has become more essential in the recent decade. The DR programs that benefit from energy-saving capabilities of flexible loads such as thermostatically controllable loads and EVs have been discussed in the literature as a cost-effective solution. The main target of these studies was to maintain the flexibility and reliability of power grid and to ensure that the residential end-users satisfy their energy demands on their own. In [4], a mathematical model that aims to increase the distribution system reliability for a system structure involving on-site photovoltaic (PV) units and DR strategies was proposed. The authors of [5] examined the impacts of real-time price-based DR application on the system reliability by considering the nodal price uncertainties and potential flexibility without renewable energy system (RES)-based production. A security constraint unit commitment model was presented in [6] by integrating a DR program and considering RESs where the system was modeled through a multi-objective problem by considering the efficiency of the market, system reliability and air pollution. The authors of [7] studied on the smart homes participated in a DR program and developed a smart home integrated management model based on a non-dominated sorting genetic algorithm to reduce the peak load and electricity costs. To evaluate the influence of smart homes on the distribution grid, various electricity appliances were involved in the study by considering different types of householder behaviors. Furthermore, the regions with and without a time-of-use tariff were compared, demonstrating that the time-of-use tariff outperforms the no-time-of-use tariff. In a similar study, a direct load control (DLC) approach was presented to improve the power system operations in terms of willingness of end users to participate in the DLC-based DR program [8]. To increase the participation of the end users of residential heating, ventilation and air conditioning units, an incentive mechanism based on providing energy credits was used. However, the RES-based production was not included in studies [7, 8] and energy storage systems (ESSs) were not considered in studies [4-8]. In [9] and [10], an optimal energy management model for an EV parking lot (EVPL) was proposed by considering the peak load reduction (PLR)-based DR programs to enhance the power system flexibility and maximize the load factor of EVPL. The uncertain behavior of EVs was also taken into account by considering the real historical data. Nevertheless, the RES-based production and ESSs were not investigated in both studies.

The applicability and efficiency of the DR programs can be improved to a greater extent when they are implemented within a microgrid that includes ESSs. Furthermore, the large-scale energy storage units have been widely regarded as one of the most effective backup assets for the power system operations, especially when using with RESs that have intermittent and non-dispatchable nature. None of the aforementioned studies, however, has considered these large-capacity ESSs. In [11], a shared energy storage control policy was developed based on the real historical data to minimize the electricity cost of the residential consumers while taking into account the stochastic nature of load demand, solar power production and time-varying electricity price. An energy management approach was developed in [12] for controlling the energy exchanges between the PV generation,

ESS and EV charging station (EVCS). However, the DR programs and Vehicle-to-Grid (V2G)/Vehicle-to-Home (V2H) services were not taken into account in both studies. Authors of [13] proposed a multi-objective scheduling problem for a smart microgrid including wind turbines (WT), diesel generators and ESSs, and studied on the service pricing and load scheduling with the aims of minimizing the operation cost, carbon emission, load curtailment cost and deviation between the power generation of WTs and demand profile. A stochastic energy management framework for a microgrid consisting of PV systems and ESS was proposed in [14] to minimize the energy cost. A 15-node radial distribution network was used in the study to evaluate the stochastic energy management framework, which was formulated as mixed integer non-linear programming. As a result, the comparative case studies validated the effectiveness of the DR strategy and ESS as a cost-effective solution. Besides, a detailed comparison analysis based on RESs, diesel generator and ESSs was conducted in [15] by taking a DR program into account to determine the optimal capacity and techno-economic benefits of a standalone microgrid. The simulation results showed that PV plus ESS is the most economical configuration. In [16], an energy management strategy for a residential area including RESs and detached houses was discussed by using an energy credit based-DR program with a shared ESS. An optimization problem was developed to minimize the energy costs of end users and reduce the peak demand in a dynamic price environment. Nevertheless, none of the aforementioned studies has considered the V2G/V2H services.

In addition to the ESSs, the potential of the EVs as energy storage units were also investigated in the recent literature by making use of the V2G technology that enables the bidirectional power flow between the EV battery and power grid [17]. This technology enables EVs to be used as both a flexible demand source and a storage option in smart grids [18]. In the literature, many technical and economic studies have been carried out to ensure the flexibility and reliability of the power system by using the V2G and V2H services. In [19], a performance evaluation method was proposed to show the impacts of EVs and V2G service on shaving the peak demand and filling the valley demand at different penetration levels of EVs and V2G. According to the case studies, the analyses indicated that charging EVs at late night or early morning would be best option for PLR. However, the effects of EV charging and V2G service were not investigated by using the DR programs and the EV battery degradation was not addressed. The authors of [20] presented a distributed resource allocation approach with a large number of plug-in EV connected to a microgrid considering the charging/discharging patterns. The main purpose of this study was the load profile smoothening and minimizing of load shifting; however, DR programs and any battery degradation model were not handled in this study. A flexibility evaluation method for distribution systems was propounded in [21], which is based on RESs and charging/discharging control strategy of EVs. In the study, the battery capacity, driving plan of EV and traffic network were modeled; however, neither DR programs nor battery degradation model were examined.

In [22-26], the potential benefits of the V2G and V2H services were investigated by considering the battery degradation of EVs. The authors of [22] presented an electricity supply cost model to reduce the total electricity cost by integrating the EVs into the

power system in China and investigated the load demand and electric supply cost under three charging operation modes, namely, random charging, controlled charging and V2G charging. Since the analysis is based on the existing fixed tariff in China, neither DR strategies nor real-time tariffs were not taken into account. The use of the V2G service has provided a relative profit in the fixed tariff environment along with the battery degradation cost. Authors of [23] and [24] presented bidirectional V2G operation methods to provide the frequency regulation service while in [25] a home energy management system was proposed by using the EV batteries. In the three studies above, the technical and economic benefits on the power system were assessed using only three different EV data and in terms of only the bidirectional V2G/V2H services. Thus, RES-based production, ESSs and DR based programs were not taken into account. Authors of [26] suggested a model in which EVs are charged at home in the evening and power is delivered to the grid via V2G service at the workplace during the day with the aim of peak shaving and valley filling. The economic and environmental benefits of a city-scaled V2G model were analyzed while including battery degradation but not DR strategies.

Table 1 presents a comprehensive comparison of the recent studies in this area to show the main contributions of this study. As seen from the table, this study differs significantly from the existing literature, particularly in that it considers both the energy credit mechanism (ECM) and EV charging/discharging using V2G/V2H technologies with battery degradation. Unlike the previous studies, the ECM has been modified to serve a microgrid that comprises a shared ESS, an EV fleet and rooftop PV systems. Due to the uncertain behavior of the EV users and the different charge/discharge characteristics of EVs from residential loads, two separate ECMs have been developed, one for the shared ESS and one for the EV fleet.

1.2 Contribution

In this study, an energy management model is developed in a linear programming framework by using a shared ESS and an EV fleet with the aim of providing the flexibility and reliability to the power system operation and also economic benefits to the end-users.

The contributions of this study are as follows:

- An energy management strategy based on a shared ESS and V2G/V2H services is propounded to serve a grid-connected neighborhood including residential end-users with rooftop PV systems and EVs.
- Novel ECMs have been developed separately for the shared ESS and V2G/V2H services to allocate the benefits from these services fairly.
- The uncertainties belonging to the EV users, which are the unpredictable departure/arrival times and initial state-of-energy (SoE) of EVs, are derived randomly using Weibull distribution and normal distribution method, respectively. Also, the DR event and V2G/V2H services start at certain time steps with regard to the last arrival time to maintain the fairness between the end-users.

- A realistic battery degradation cost estimation model is proposed by considering the salvage value contrary to the studies in the literature.

The rest of the paper is organized as follows. The system description and formulation of the proposed energy management model are presented in Section II. Afterwards, the acquired input data, the case studies evaluated and simulations are examined in Section III. Finally, the conclusion and future work are described in the last section.

Table 1. Taxonomy of the proposed method compared to similar studies

Ref.	DR strategy	Time varying pricing	ECM	RES based production		Large-Scale ESS	EV controlled charging	V2G/ V2H	Battery Degradation	Point of view	
				PV	WT					LSE	End-user
[4]	✓	-	-	✓	-	-	-	-	-	✓	✓
[5]	✓	✓	-	-	-	-	-	-	-	✓	✓
[6]	✓	✓	-	-	✓	-	-	-	-	✓	-
[7]	✓	✓	-	-	-	-	-	-	-	✓	✓
[8]	✓	✓	✓	-	-	-	-	-	-	✓	✓
[9]	✓	-	-	-	-	-	✓	-	-	✓	-
[10]	✓	-	-	-	-	-	✓	-	-	✓	✓
[11]	-	✓	-	✓	-	✓	-	-	-	-	✓
[12]	-	-	-	✓	-	✓	✓	-	-	✓	-
[13]	✓	✓	-	-	✓	✓	-	-	-	-	✓
[14]	✓	✓	-	✓	-	✓	-	-	-	✓	-
[15]	✓	✓	-	✓	✓	✓	-	-	-	✓	-
[16]	✓	✓	✓	✓	-	✓	-	-	-	✓	✓
[19]	-	-	-	-	-	-	✓	✓	-	✓	-
[20]	-	-	-	-	-	-	✓	✓	-	✓	✓
[21]	-	-	-	✓	-	✓	✓	✓	-	✓	-
[22]	-	-	-	-	-	-	✓	✓	✓	✓	-
[23]	-	✓	-	-	-	-	-	✓	✓	✓	✓
[24]	-	-	-	-	-	-	✓	✓	✓	✓	✓
[25]	-	✓	-	-	-	-	✓	✓	✓	✓	✓
[26]	-	✓	-	✓	✓	-	✓	✓	✓	✓	✓
This study	✓	✓	✓	✓	-	✓	✓	✓	✓	✓	✓

Note: LSE = Load Serving Entity.

2. Methodology

2.1 System Description

In this study, a grid-connected microgrid including a neighborhood composed of residential end-users with rooftop PV systems, an EV fleet, an EVCS with V2G/V2H technology and a large-capacity ESS is considered, as shown in Fig. 1. It can be seen from the system scheme that three different power exchanges are available in the microgrid: between the houses and grid/neighborhood, between the shared ESS and grid/neighborhood, and between the EV fleet and grid/neighborhood. The houses provide their energy demand primarily from their PV systems while the residual demand can be provided from the surplus PV power of the other houses (which will be referred to local power hereafter). When the PV power is insufficient to satisfy all the required demands, additional power may be purchased from the grid or drawn from the shared ESS and EV fleet. On the contrary, the excess PV production, if any, can be sold to the grid or delivered to the shared ESS. In a typical moment, the decision of whether purchasing or selling energy will be made by the energy management system depending on various parameters such as EV departure/arrival times, energy credits and dynamic prices. Also, the neighborhood transformer is assumed to have a load tracking system that prevents the overloading on the transformer windings so that may help to decelerate the aging process.

2.2 Mathematical Model

2.2.1 Battery Degradation

In this study, the cost of delivering electricity from an EV to the power grid or to the houses by V2G and V2H services is determined by estimating the battery degradation. Also, when calculating the degradation, the capital cost (CC) of the battery is taken into account, together with the salvage value of the battery once it has run its course. The battery degradation cost of EV is defined in (1) [25], [27]:

$$C_e^{deg} = \frac{(C_{unit} \times \sigma) + C_{labor} - SV}{N_{cycle} \times \sigma \times DoD} \tag{1}$$

A deep discharge (*DoD*) is typically suggested as 80% for li-ion batteries [23]. In addition, the cycle life of a battery (*N*), which is for a specific *DoD*, is a measurement of how many charge-discharge cycles the battery can withstand before losing its capacity. C_{unit} and C_{labor} are taken as 137 $/kWh and $168 [25] while C_{unit}, C_{labor} and σ represent the battery cost per kWh, battery replacement labor cost and EV battery capacity, respectively. Thus, CC is equal to $C_{unit} \times \sigma$. *N* is 3221 cycles at 80% *DoD* as reported in [28]. The salvage value of the battery is denoted by SV in (1), which is adapted from [29] as equal to 60% of the CC. Hence, the battery degradation cost per kWh varies according to the EV battery capacities given in Table 2 and is estimated as an average of $0.0225. As a result, it is taken into account in the objective function of the proposed optimization problem while calculating the total energy cost of the households (TEC).

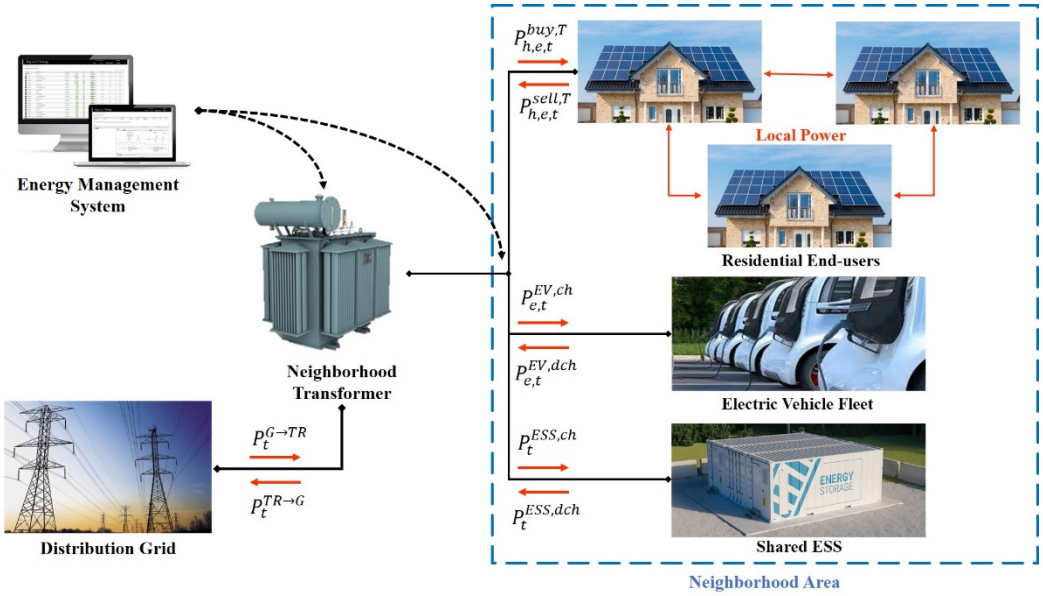

Figure 1. The schematic diagram of the system proposed.

Table 2. Electrical characteristics of electric vehicles

EV Type	Battery Cap. [kWh]	EV Type	Battery Cap. [kWh]
BMW i-3	37.9	Tesla Model 3	75
Hyundai Kona	64	Kia E-Niro	64
Mini Cooper Se	28.9	Audi Q4 E-Tron	76.6
Mercedes Eqc 4matic	80	Hyundai Kona Limited	39
Renault Zoe	52	Volvo Xc40	75

2.2.2 *Objective Function*

The objective function of the defined optimization problem is determined as the minimization the TEC as shown in (2).

$$TEC = \sum_{h\in H, e\in E, t\in T} (\lambda_t^{buy} \times \left(P_{h,t}^{buy,G} + P_{h,t}^{buy,L} + P_{e,t}^{G\to EV}\right) - \lambda_t^{sell} \times \left(P_{h,t}^{sell,G} + P_{h,t}^{sell,L} + P_{e,t}^{EV\to G}\right) + (C_e^{deg} \times P_{e,t}^{EV,dch})) \times \Delta T \quad (2)$$

2.2.3 *Power Constraints*

As shown in (3), the amount of power provided to each house at a certain time is divided into four components: $P_{h,t}^{buy,L}$ defines the power provided from surplus PV power of other houses to house h while $P_{h,t}^{buy,G}$ denotes the power purchased from the grid, then $P_{h,t}^{buy,ESS}$ and $P_{e,t}^{buy,EV}$ are the power supplied from shared ESS and EV e respectively. Similarly, the amount of power provided by each house at a given moment consists of four components as in (4): $P_{h,t}^{sell,L}$ defines the power provided from house h to other

houses while $P_{h,t}^{sell,G}$ denotes the power sold from house h to the grid, then $P_{h,t}^{sell,ESS}$ and $P_{e,t}^{sell,EV}$ are the power transferred from house h to the shared ESS and EV e respectively. In addition, (5) expresses that the total received and transferred local power within the neighborhood should be equal to each other in time period t in order to maintain a balance of the purchased and sold energy between the houses in the neighborhood. (6) states the power consumed by the neighborhood from the transformer whereas (7) designates the power sold by the houses in the neighborhood via transformer. Constraint (8) represents the power flow from the grid to the neighborhood, ESS and EVs through the transformer. In constraint (9), on the other hand, the power flowed to the grid through the transformer is shown. The total power flow through the transformer is limited by (10) and (11). Besides, the bidirectional power flow is prevented by the binary variable in (10) and (11) since the bidirectional power flow is unavailable in the same time period for transformers.

$$P_{h,e,t}^{buy,T} = P_{h,t}^{buy,G} + P_{h,t}^{buy,L} + P_{h,t}^{buy,ESS} + P_{e,t}^{buy,EV}, \forall\, h, e, t \tag{3}$$

$$P_{h,e,t}^{sell,T} = P_{h,t}^{sell,G} + P_{h,t}^{sell,L} + P_{h,t}^{sell,ESS} + P_{e,t}^{sell,EV}, \forall\, h, e, t \tag{4}$$

$$\sum_{h \in H} P_{h,t}^{buy,L} = \sum_{h \in H} P_{h,t}^{sell,L}, \forall\, t \tag{5}$$

$$\sum_{h \in H} P_{h,t}^{buy,G} = P_t^{G \to N}, \forall\, t \tag{6}$$

$$\sum_{h \in H} P_{h,t}^{sell,G} = P_t^{N \to G}, \forall\, t \tag{7}$$

$$P_t^{G \to TR} = P_t^{G \to N} + P_t^{G \to ESS} + \sum_{e \in E} P_{e,t}^{G \to EV}, \forall\, t \tag{8}$$

$$P_t^{TR \to G} = P_t^{N \to G} + P_t^{ESS \to G} + \sum_{e \in E} P_{e,t}^{EV \to G}, \forall\, t \tag{9}$$

$$P_t^{G \to TR} \leq P^{TR} \times b_t^1, \forall\, t \tag{10}$$

$$P_t^{TR \to G} \leq P^{TR} \times (1 - b_t^1), \forall\, t \tag{11}$$

The formulation of shared ESS model is depicted by (12)-(20). Constraints (12) and (13) limits the charge and discharge capacities of the shared ESS. Furthermore, the binary variable in (12) and (13) prevents the shared ESS from being charged and discharged at the same time period. Equation (14) expresses the SoE of the shared ESS while the SoE at each time period is limited by the minimum and maximum SoE values in (15). The initial SoE of the shared ESS is determined by (16). The battery is charged by the power drawn from the neighborhood and drawn from the grid through neighborhood transformer as represented in (17). Similarly, (18) shows that the shared ESS is discharged by the power transferred from the shared ESS to the houses in the

neighborhood and to the power grid. Finally, (19) and (20) represent the total purchased power from ESS and the total sold power to the ESS by the neighborhood, respectively.

$$0 \le P_t^{ESS,ch} \le P_{ESS}^{CH} \times b_t^2, \forall\, t \tag{12}$$

$$0 \le P_t^{ESS,dch} \le P_{ESS}^{DCH} \times (1 - b_t^2), \forall\, t \tag{13}$$

$$SOE_t^{ESS} = SOE_{t-1}^{ESS} + \eta^{CH} \times P_t^{ESS,ch} \times \Delta T - P_t^{ESS,dch} / \eta^{DCH} \times \Delta T,\ \forall\, t;\ \ if\ t > 1 \tag{14}$$

$$SOE^{ESS,min} \le SOE_t^{ESS} \le SOE^{ESS,max}, \forall\, t \tag{15}$$

$$SOE_t^{ESS} = SOE^{ESS,0},\quad if\quad t = 1 \tag{16}$$

$$P_t^{ESS,ch} = P_t^{N \to ESS} + P_t^{G \to ESS}, \forall\, t \tag{17}$$

$$P_t^{ESS,dch} = P_t^{ESS \to N} + P_t^{ESS \to G}, \forall\, t \tag{18}$$

$$P_t^{ESS \to N} = \sum_{h \in H} P_{h,t}^{buy,ESS}, \forall\, t \tag{19}$$

$$P_t^{N \to ESS} = \sum_{h \in H} P_{h,t}^{sell,ESS}, \forall\, t \tag{20}$$

The formulation of EV charge-discharge model is described by the constraints (21)-(27). The constraints (21) and (22) limit the charging and discharging powers of EVs, respectively. However, the binary variables at (21) and (22) allow only one-direction power flow from or to each EV. Equation (23) represents the SoE of the EVs while SoE of each EV is limited at maximum 100% and minimum 20% by (24) to prevent the overcharge and deep of discharge.

Constraint (25) states that at the arrival time, SoE of each EV is equal to its initial value. The power balance between EVs and the transformer or neighborhood for charging and discharging EVs is shown in constraints (26) and (27).

$$0 \le P_{e,t}^{EV,ch} \le P_{EV}^{CH} \times b_{e,t}^3, \forall\, t \tag{21}$$

$$0 \le P_{e,t}^{EV,dch} \le P_{EV}^{DCH} \times \left(1 - b_{e,t}^3\right), \forall\, t \tag{22}$$

$$SOE_{e,t}^{EV} = SOE_{e,t-1}^{EV} + \eta^{CH} \times P_{e,t}^{EV,ch} \times \Delta T - P_{e,t}^{EV,dch} / \eta^{DCH} \times \Delta T, \forall\, t;\ if\ \ t > 1 \tag{23}$$

$$SOE_e^{EV,min} \le SOE_{e,t}^{EV} \le SOE_e^{EV,cap}, \forall\, e, t \tag{24}$$

$$SOE_{e,t}^{EV} = SOE_e^{EV,0}, \forall\, e;\ if\ t = T_{arr} \tag{25}$$

$$P_{e,t}^{EV,ch} = P_{e,t}^{N \to EV} + P_{e,t}^{G \to EV}, \forall\, e, t \tag{26}$$

$$P_{e,t}^{EV,dch} = P_{e,t}^{EV \to N} + P_{e,t}^{EV \to G}, \forall\, e, t \tag{27}$$

The power constraints of each house are shown by (28)-(31). Constraint (28) provides the balance between load demand and power supplied from grid and PV system. With the binary variables in constraints (29) and (30), the houses can either deliver power to or draw power from the grid at each time period since the unavailability of a bidirectional power flow in the same time period. Equation (31) states that the PV power generation can be utilized by the houses and surplus power, if any, is delivered to the power grid in order to gain profit.

$$P_{h,e,t}^{buy,T} + P_{h,t}^{PV,used} = LD_{h,t}\ , \forall\ h, e, t \tag{28}$$

$$P_{h,e,t}^{buy,T} \leq N \times b_{h,e,t}^{4}\ , \forall\ h, e, t \tag{29}$$

$$P_{h,e,t}^{sell,T} \leq N \times \left(1 - b_{h,e,t}^{4}\right), \forall\ h, e, t \tag{30}$$

$$P_{h,t}^{PV,used} + P_{h,e,t}^{sell,T} = P_{h,t}^{PV}, \forall\ h, e, t \tag{31}$$

2.2.4 Energy Management Strategy

The primary target of the proposed strategy is to schedule the use of both the shared ESS and EV batteries and to exploit their potential in terms of providing distribution system flexibility and reducing the energy costs of end-users. When the PV-integrated residential end-users are considered, the PV power production rarely coincides with the peak demand of the houses. Besides, assuming a dynamic price tariff is imposed in a residential area, the peak price of electricity usually occurs naturally during peak hours. Consequently, as the PV production does not coincide with peak price period, it is obvious that the excess PV energy is usually sold back to power grid at lower prices and energy demand is met by power grid with higher prices.

To overcome the aforementioned problem by integrating an ESS unit into the system, the excess PV power produced during the day is stored in the ESS unit and used during peak hours. Thus, the end-users exploit the PV system better and reduce their energy costs.

In the proposed system, each household in the neighborhood gains energy credits as much as the total energy it sent to the neighborhood, to shared ESS and to the grid until it reaches the credit limit designated by the Load Serving Entity (LSE) through the ECM. With this ECM implemented, the end-users can use the credits during peak hours to satisfy the energy demand through the DR program, which is provided by the LSE and assumed to be participated by each household.

On the other hand, it is considered that the households have EVs of different model and battery capacity in this study. In the proposed strategy, a part of the residual energy demand is met by the EV batteries rather than purchasing energy from the power grid. The V2G and V2H services, which are profitable for both the EV user and the LSE, aim to reduce the peak load by delivering the energy in the EV batteries to the power grid or the houses. These services are suitable for use in PLR-based DR applications as the arrival time of EVs to the EVCS and the peak hours generally coincide. The LSE manages the EV fleet so that it discharges during peak hours using the DR program and V2G/V2H capability, and charges during off-peak hours.

The formulation of the energy management strategy is expressed by (32)-(45). Energy credit of each house varies by transferring energy to the shared ESS or drawing energy from it, as shown in constraint (32). The initial energy credit of each house at first time step is determined by (33). The energy credit obtained by each house is limited by (34) depending on the PV system capacity and SoE of shared ESS as defined in constraint (35). In order for each household to be able to use all of their energy credits during the DR event, the shared ESS's battery capacity should be greater than or equal to the total energy credit plus the shared ESS's minimum SoE level at the beginning of the DR event, as expressed in (36). On the other hand, the energy credit of each EV varies depending on the transferred energy from or to EV batteries as shown in constraint (37) while constraint (38) defines the initial energy credit value of each EV at the start of the DR event.

Moreover, constraints (39)-(45) are designed to exploit the shared ESS and EV batteries. Constraints (39) and (40) prevent the energy transfer to the shared ESS during DR period and from the shared ESS to the neighborhood during outside the DR period, respectively. Constraints (41) and (42) prevent the charging of the EVs during the DR period while constraints (43) and (44) prevent the discharging of the EVs outside the DR period. Finally, constraint (45) requires that each EV batteries charge to 100% SoE until the next day.

$$E_{h,t}^{Crd} = E_{h,t-1}^{Crd} + \left(P_{h,t}^{sell,ESS}\right) \times \Delta T - \left(P_{h,t}^{buy,ESS}\right) \times \Delta T \,, \forall\, h, t; \;\; if \;\; t > 1 \tag{32}$$

$$E_{h,t}^{Crd} = E_{h}^{Crd,0}, \forall\, h; \;\; if \;\; t = 1 \tag{33}$$

$$E_{h,t}^{Crd} \leq E_{h}^{Crd,max}, \forall\, h, t \tag{34}$$

$$E_{h}^{Crd,max} = (SOE^{ESS,max} - SOE^{ESS,0}) \times PV_{h}^{cap} / PV^{cap,tot} \,, \forall\, h \tag{35}$$

$$SOE_{t}^{ESS} \geq \sum_{h \in H} E_{h,t}^{Crd} + SOE^{ESS,min}, \qquad if \;\; t = T^{DR.start} \tag{36}$$

$$E_{e,t}^{Crd,EV} = E_{e,t-1}^{Crd,EV} + \left(P_{e,t}^{sell,EV}\right) \times \Delta T - \left(P_{e,t}^{buy,EV}\right) \times \Delta T \,, \forall\, e, t; \;\; if \;\; t \geq T^{DR,start} \tag{37}$$

$$E_{e,t}^{Crd,EV} = E_{e}^{Crd,EV0}, \forall\, h; \;\; if \;\; t = T^{DR,start} \tag{38}$$

$$P_{h,t}^{sell,ESS} = 0, \forall\, h, t \;\in [T^{DR,start}, T^{DR,end}] \tag{39}$$

$$P_{h,t}^{buy,ESS} = 0, \forall\, h, t \;\notin [T^{DR,start}, T^{DR,end}] \tag{40}$$

$$P_{e,t}^{sell,EV} = 0, \forall\, e, t \;\in [T^{DR,start}, T^{DR,end}] \tag{41}$$

$$P_{e,t}^{G \to EV} = 0, \forall\, e, t \;\in [T^{DR,start}, T^{DR,end}] \tag{42}$$

$$P_{e,t}^{buy,EV} = 0, \forall\, e, t \;\notin [T^{DR,start}, T^{DR,end}] \tag{43}$$

$$P_{e,t}^{EV \to G} = 0, \forall\, e, t \;\notin [T^{DR,start}, T^{DR,end}] \tag{44}$$

$$SOE_{e,t}^{EV} = SOE_{e}^{EV,cap} \; if \;\; t = T^{end} \tag{45}$$

3. Test and Results

3.1 Input Data

PV power production and load demand measurements belonging to a set of houses in a region Austin, TX, USA were obtained from [16]. High PV power production potential of the location and the availability of the high-resolution data (i.e., recorded for each five minutes) are the key factors in selecting this dataset. The data of 40 detached houses are selected from this region and assumed that the houses compose a neighborhood with their own solar panels and EVs. The energy consumption and PV production of the neighborhood are demonstrated together in Fig. 2. When considering the variation of PV production and load demand of the houses, it remarks that the supply and demand data do not usually overlap with each other, which implies that the neighborhood can be a good environment to implement a shared ESS. Since battery sizing and cost are beyond the scope of this study, it is assumed that a shared ESS of 300 kWh is deployed in the microgrid, considering the worst case when there is an overloading on the power grid with very limited sunlight. Nevertheless, the battery capacity is increased or decreased by ±50% in the case studies to demonstrate the effects of the shared ESS with different capacities on the results. Besides, it should be stated that a real-time pricing tariff adopted from [16] is utilized for the electricity price, as shown in Fig. 3.

Also, the most popular ten EV models in the market that have 11 kW charging rate through Type-2 EVCS are considered in the study in order to achieve more realistic assessments, as demonstrated in Table 1 [30]. It is assumed that the Type-2 EVCS provides the maximum charging/discharging power of 22 kW and a charging/discharging efficiency of 0.98 [31]. Finally, the key parameters for the constituents employed in the proposed system are listed in Table 3 and Table 4.

The EV departure/arrival behavior and the initial SoE of EVs (at the arrival time of EVs at the EVCS) are some uncertainties in the EV charging/discharging model. In order to obtain stochastic EV departure/arrival times, two-parameter Weibull distribution is applied by adapting the original data from [9]. Two-parameter Weibull distribution function is expressed by (46) in which x is the time bin, α and β are the shape and the scale parameters, respectively.

$$F(x) = 1 - e^{-(\frac{x}{\beta})^{\alpha}} \tag{46}$$

Table 3. Key parameters of the proposed system

Constituents	Parameters	Initial Value	Minimum Value	Maximum Value	Units
Neighborhood Transformer	P^{TR}	-	-	2000	kW
PV System	PV_h^{cap}	-	5	11	kW
	$PV^{cap,tot}$	-	-	285	kW
EV Fleet	P_{EV}^{CH}/P_{EV}^{DCH}	-	-	11	kW
	C_e^{deg}	-	0.0221	0.0235	$/kWh
	SOE_e^{EV}	9.7-53.1*	5.8-16	28.9-80	kWh
	E_e^{Crd}	1.8-37.1*	0	1.8-37.1	kWh

Note: *= at starting of DR event (7:00 p.m.)

Table 4. Key parameters of the shared ESS for various case studies.

Parameters	Initial Value			Minimum Value			Maximum Value			Units
	Case 2 & 4	Case 1,3 & 5	Case 6	Case 2 & 4	Case 1,3 & 5	Case 6	Case 2 & 4	Case 1,3 & 5	Case 6	
$P_{ESS}^{CH}/P_{ESS}^{DCH}$	-	-	-	-	-	-	30	60	90	kW
SOE^{ESS}	75*	150*	225*	30	60	90	150	300	450	kWh
E_h^{Crd}	0*	0*	0*	0	0	0	2.1-4.6	4.2-9.3	6.3-13.9	kWh

Note: * = at starting of day (7:00 a.m.)

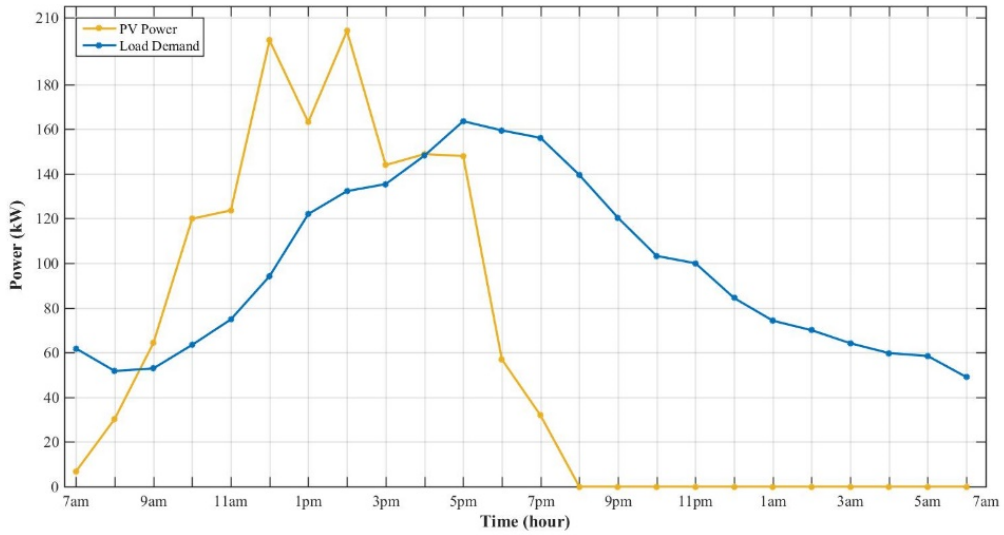

Figure 2. PV power output and load demand in a test period of one day.

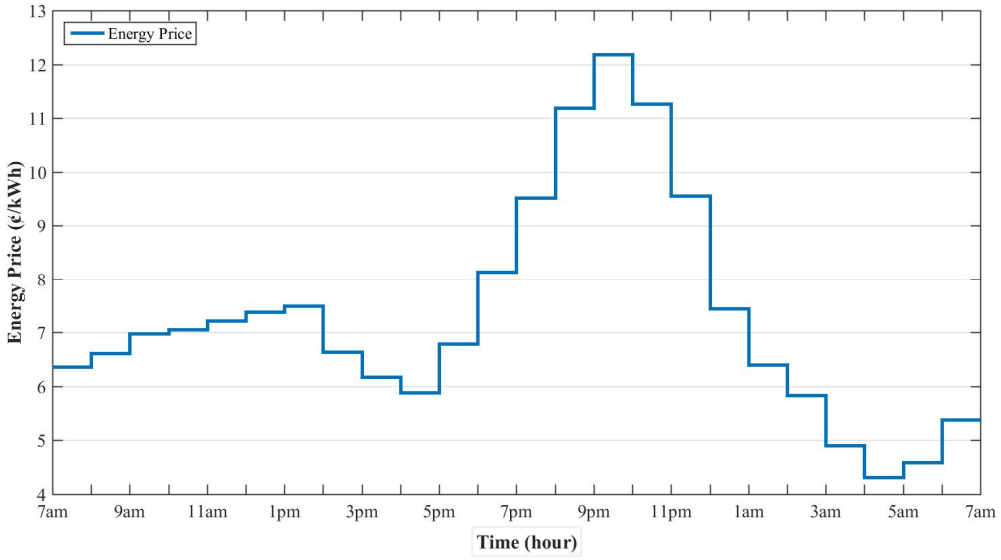

Figure 3. Price variation in a test period of one day.

Appropriate α and β values are found by using MATLAB *dfittool* as 1.59 and 4.08 for departure, and 1.47 and 4.04 for arrival, respectively. Figure 4 shows the departure/arrival times distribution with 15-minute time intervals for departure from 7am to 9:30am and for arrival from 4:30 p.m. to 7 p.m. It should be stated that a weekday when EV users leave their houses in the early morning and arrive at EVCS at the end of the working hours is considered in the proposed strategy. Accordingly, the starting and ending times of one day test period are determined as 7:00 a.m. and 6:59 a.m., respectively. In addition, the DR event period is determined between 7 p.m. and 11:00 p.m., considering the EVs' arrival times and peak load demand hours. On the other hand, the initial SoE level of each EV is obtained randomly using normal distribution as represented in Fig. 5. Mean and standard deviation values are defined as $\mu = 50\%$ and $\sigma = 9.55\%$, respectively. It should be stated that the proposed optimization method is tested using General Algebraic Modeling System (GAMS) v.25.1.3 software and solver CPLEX. It takes 0.56s to solve the mixed integer problem using a Quad Core Laptop with 2.5 GHz CPU and 8 GB RAM.

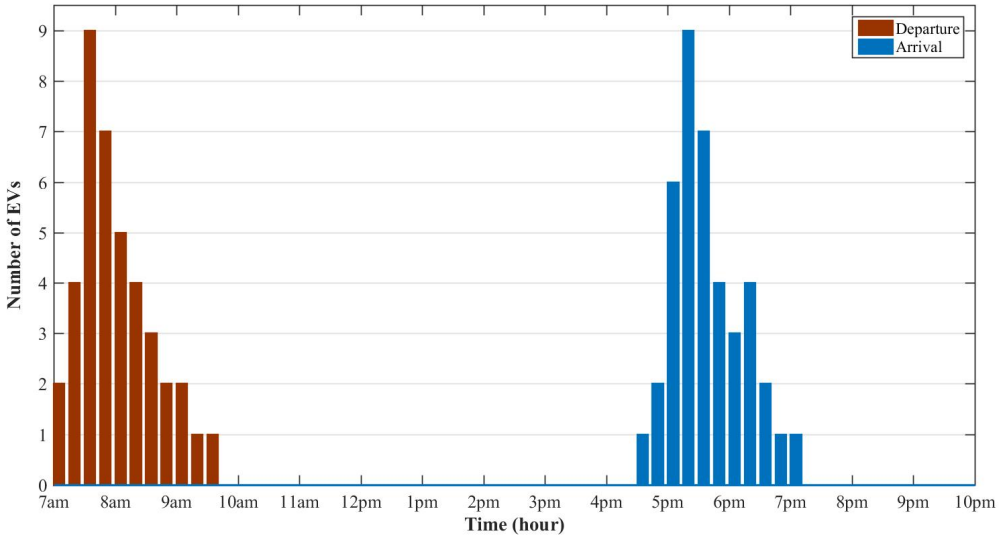

Figure 4. The departure/arrival times distribution.

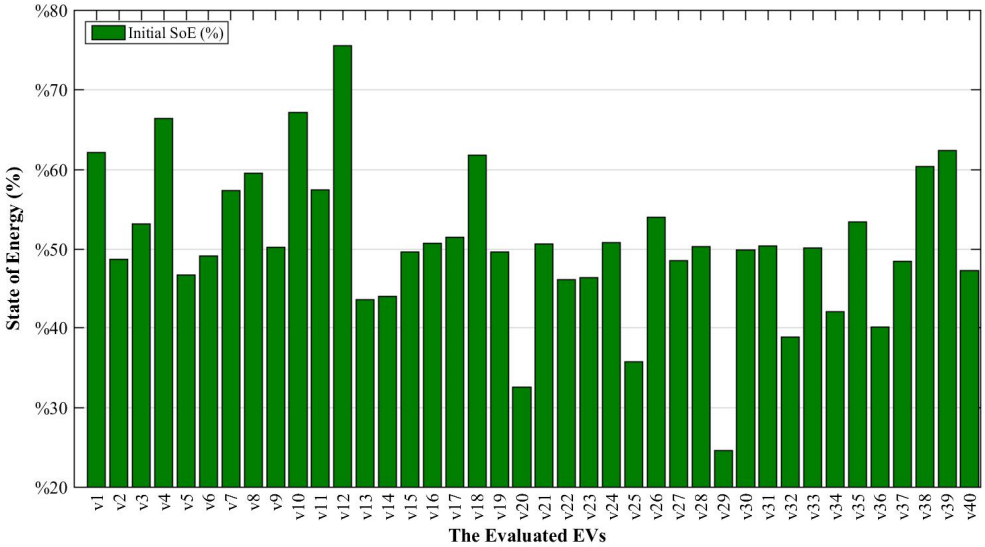

Figure 5. The initial SoE variation of EVs before V2G/V2H operation.

3.2 Simulation and Results

The effectiveness of proposed model is tested by considering a base case together with six different cases, as listed in Table 5:

Table 5. Case Studies

Cases	DR	Shared ESS	ESS-to-Grid	V2G	V2H	ECM	
						Shared ESS	EV Fleet
Base Case	-	-	-	-	-	-	-
Case 1	✓	✓ (300kWh)	✓	-	-	✓	-
Case 2	✓	✓ (-50%)	-	-	✓	✓	✓
Case 3	✓	✓ (300kWh)	-	-	✓	✓	✓
Case 4	✓	✓ (-50%)	✓	✓	✓	✓	✓
Case 5*	✓	✓ (300kWh)	✓	✓	✓	✓	✓
Case 6	✓	✓ (+50%)	✓	✓	✓	✓	✓

Note: *= Proposed Case

First, in order to evaluate the potential benefits of the proposed method, V2G and V2H are not included in the first two cases and therefore only the charging schedule of EVs is considered in these cases. Since there is no energy management strategy, the Base Case can be considered as the worst case. In this case, the houses use their own PV energy first, then purchase the grid power if their production is less than their demand. Houses must satisfy their demand from grid during the peak price hours as the PV production is unavailable in the evening and nighttime. Figure 6 shows the variation of grid power and PV power consumed in the neighborhood for Case 1. In the first case, the houses first utilize their own PV generation and use the shared surplus PV power, named local power, instead of purchasing from the grid. Excess energy, if any, is stored in the shared ESS and used by the houses via ECM during DR period.

For Cases 2-6, EVs are not considered as a load required to be charged, instead they are used as an energy storage option. Residual energy of the EV batteries is used for providing the household's energy demand during the DR period in Case 2 and Case 3. Similar to the Case 1, the houses first utilize their own PV generation and local power in the daytime. Also, during DR period the houses have a chance to exploit both shared ESS and EV fleet's batteries. On the other hand, EV users can sell their excess battery energy to the grid via the V2G service during the DR period in Cases 4, 5 and 6.

Cases 3, 4, and 6 are designed to investigate the effectiveness of the shared ESS on PLR and TEC with different battery capacities. Therefore, these cases are ignored in Fig. 7 for the sake of simplicity since their graphical results are similar to those in the cases where the shared ESS with the original capacity (300 kWh) is used. For Cases 1, 2 and 5, the local power exchanges are shown in Fig. 7. As seen in Fig. 7, the local power variations overlap from 2:00 p.m. to 6:00 p.m. contrary to Case 2. The stored

energy cannot be sold back to the grid due to the lack of bidirectional power flow for shared ESS and EV fleet in Case 2. Therefore, while the PV power transferred to the shared ESS decreases in Case 2, the local power exchange increases. The power drawn from the grid is given in Fig. 8 for four different cases. Since Case 2 has a higher local power exchange, the grid power decreases between 4:00 p.m. and 6:00 p.m. Besides, as seen in Fig. 8, the peak load demand of the purchased power from grid during the DR period is significantly reduced in Case 2 and Case 5. The use of higher grid power in Case 5 than in Case 2 is due to the fact that selling energy to the grid via V2G during the highest energy price period is more profitable than satisfying load demand in the neighborhood.

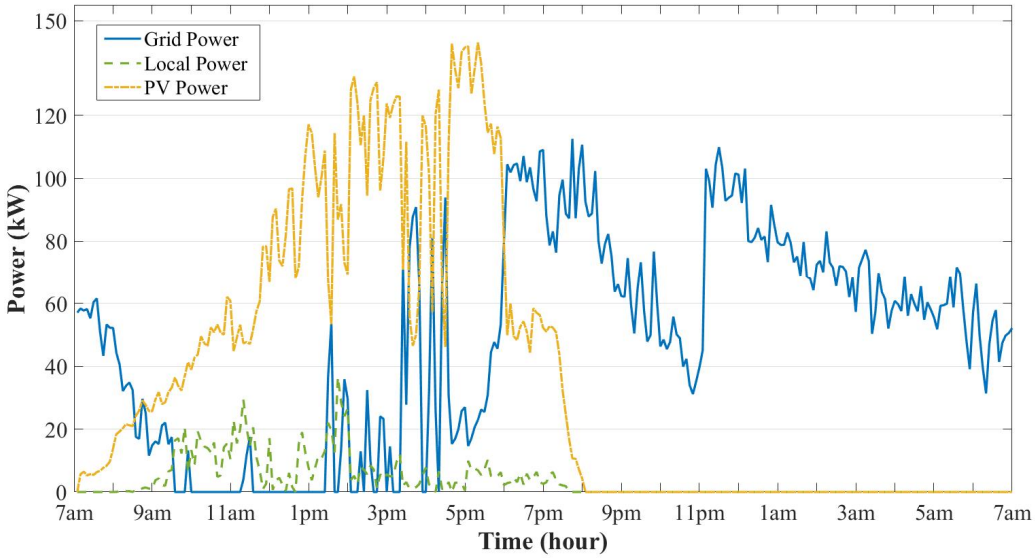

Figure 6. Power exchanges for Case 1 in a test period of one day.

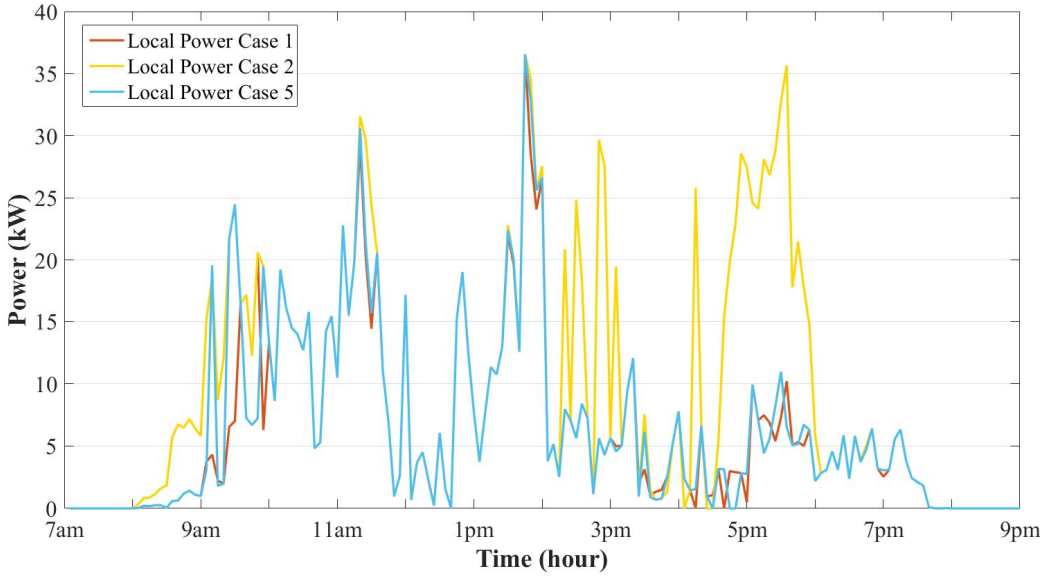

Figure 7. Local power exchange for three different cases in a test period of one day.

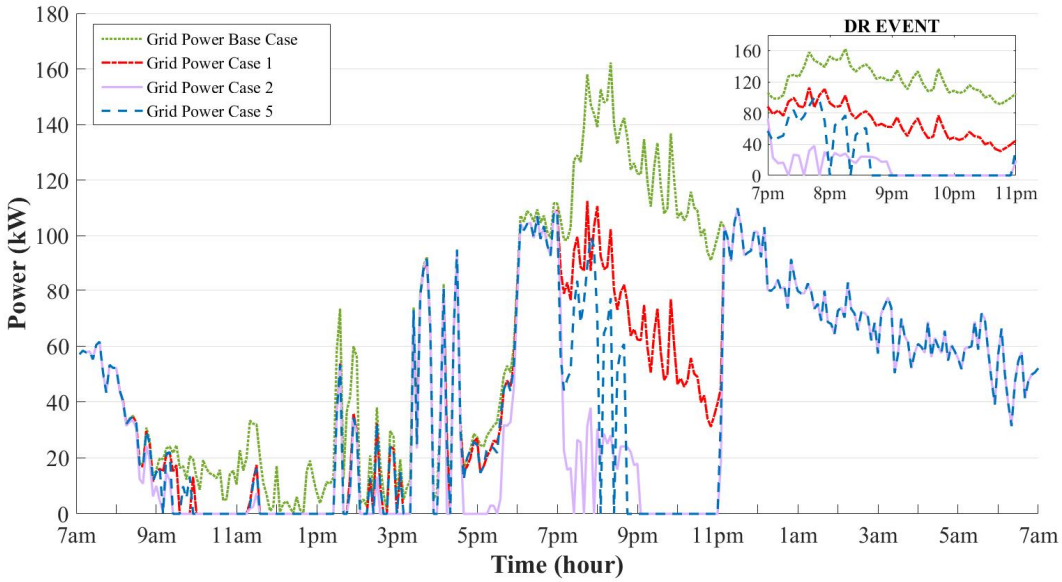

Figure 8. Grid power exchange for four different cases in a test period of one day.

The energy credits and SoE of the shared ESS are demonstrated for Cases 1 - 6 in Fig. 9. The cases with different shared ESS capacities are split into two plots to demonstrate the variations of the SoE and energy credits explicitly. It is clear from Fig. 9 that the SoE level of the shared ESS variations is similar for all the cases. This is because the shared ESS is used in all cases to minimize the TEC instead of drawing power from the grid. On the other hand, contrary to Cases 2 and 3, the power from the shared ESS sold to the grid between 10 a.m. and 2 p.m. is the reason of the ripples in the SoE. Besides, due to the small ESS capacity in Cases 2 and 4, the maximum energy credit limits are lower than the other cases as seen in Fig. 9.

Figure 10 and 11 depict the change in the SoE level and energy credits of the EV fleet, respectively, based on the departure/arrival times and EV charge/discharge behaviors for Case 2 and Case 5. In these figures, the extremum values are indicated by the top and bottom horizontal black lines, respectively, whereas the median is shown by the middle red line in the box. In addition, the first and third quartiles are shown by the horizontal blue lines below and above the median. Since V2H and V2G services are employed together in Case 5, the batteries of the EV fleet are better exploited and energy credits are used in a more effective manner, as can be seen in these two figures. In order to compare Cases 1, 2 and 5 in terms of the SoE variation of the EVs, two random EVs, namely EV-1 and EV-40, are selected. The SoE variations starting from the arrival time of EVs to the next day are shown in Fig. 12. Since the V2G/V2H services are unavailable in Case 1, only the charging operation is considered. Therefore, as can be seen in Fig. 12, the SoE of the EVs remains at its initial level until the charging operation is started. The charging operation is carried out up to the full charge level during lowest electricity price periods.

In Case 2, the EVs transfer the power of their batteries to the houses with the different percentages of the SoE during on-peak hours and then charge their batteries up to 100% as in the first case. On the other hand, in Case 5, the EVs deliver power to the

grid and houses down to 20% during on-peak hours and then fully charge them. It should be noted that due to the unavailability of V2G service for Case 2, some EVs with large battery packs, e.g., EV-40 in Fig. 12, cannot be exploited down to 20%. As the SoE variation of the Base Case is similar to the first case, and Cases 3, 4 and 6 are similar to Cases 2 or 5, these cases are neglected in the Fig. 12 for a clearer representation.

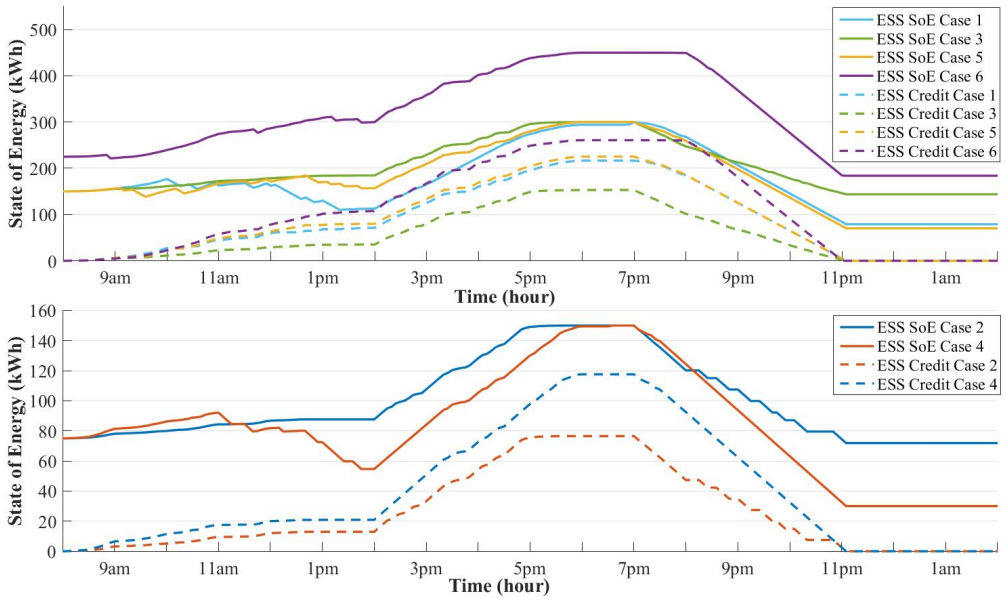

Figure 9. SoE and energy credit variation of shared ESS for all cases in a test period of one day.

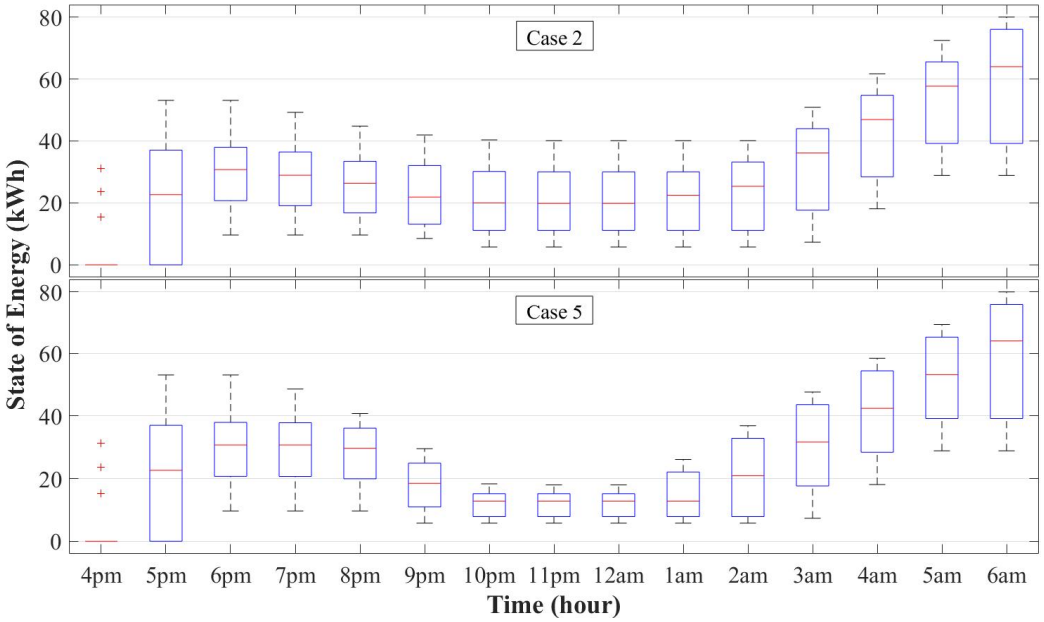

Figure 10. SoE level variation of EVs for Case 2 and 5 in a test period of one day.

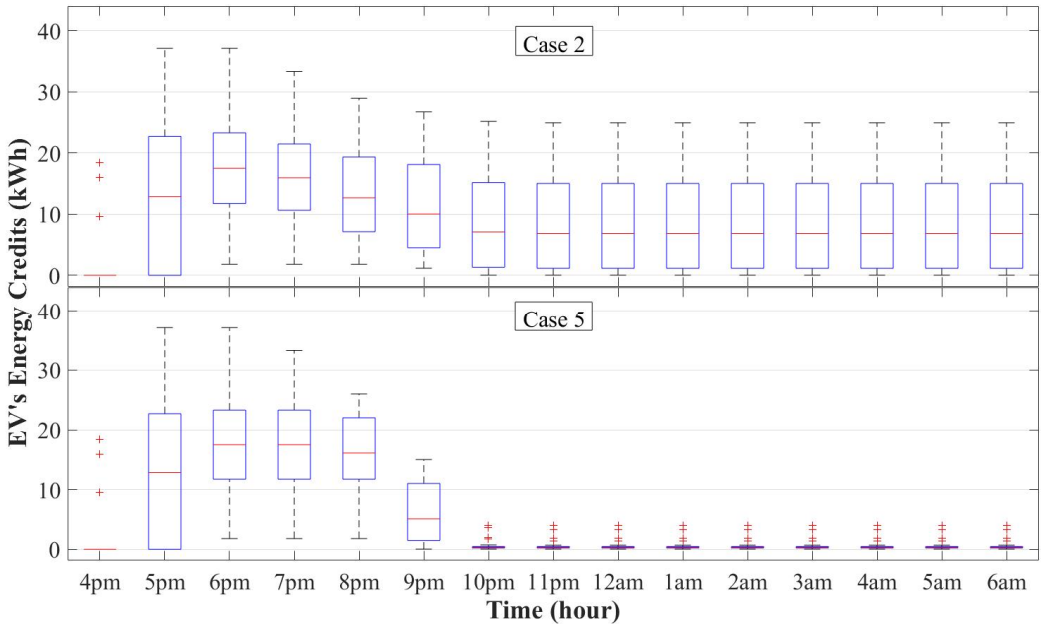

Figure 11. Energy credit variation of EVs for Case 2 and 5 in a test period of one day.

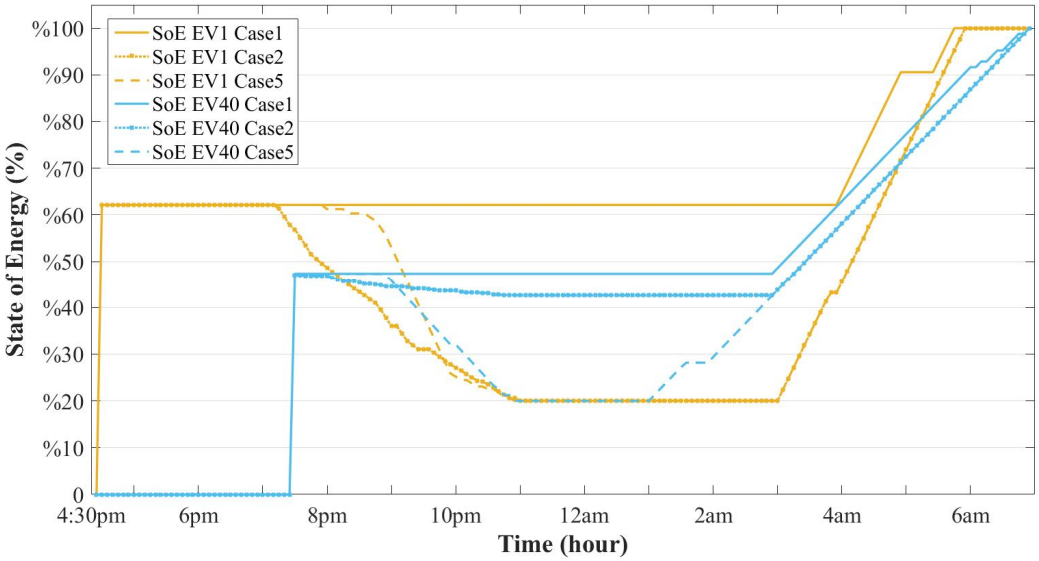

Figure 12. SoE level variation of selected EVs for Case 1, Case 2 and Case 5 in a test period of one day.

Another important result can be obtained by comparing the PLR values, which are calculated by (47) and equal to the total power provided by the ESS and EV fleet to the grid and the houses during DR event, as shown in Fig. 13. Since Case 3 has 50% more shared ESS capacity than Case 2, the utilization of EV batteries is reduced, resulting in less battery degradation and lower energy costs. However, as the stored energy cannot be sold back to the grid in Case 3, increasing shared ESS capacity has only a small impact on the PLR and TEC. On the other hand, both Cases 2 and 3 have considerable PLR value compared to Case 1 since the ECM is available for both the shared ESS and EV fleet.

$$PLR = \sum_{t} P_{t}^{ESS,dch} + \sum_{t,e\in E} P_{e,t}^{EV,dch} \quad , t \in [T^{DR,start}, T^{DR,end}] \tag{47}$$

Besides, the V2G service that is available in Cases 4, 5 and 6 provides a significant PLR compared to other cases. Due to the discharging power constraints and limited DR period, increasing shared ESS capacity by 50% in Case 6 has a small effect on both PLR and TEC, as shown in Fig. 13 and Table 6. Finally, from the view of the LSEs, the proposed approach considerably reduces the peak load demand, which is a crucial challenge during stressful conditions for the grid.

The comparison of the main results for the cases is given in Table 6. While the total purchased energy is 2648.11 kWh for the Base Case, it decreases to 2392.83 kWh, 2453.11 kWh and 2388.92 kWh for Cases 1, 2 and 3, respectively. After implementing the V2G service, the EV batteries are exploited until its minimum permissible SoE level, then recharged up to 100% SoE during off-peak hours. Thus, the purchased energy increases for Cases 4, 5 and 6 compared to Base Case while the TEC decreases. Contrary to the other cases, there is no energy sold to the grid in Base Case in which the DR event is unavailable. Only the excess PV energy can be sold directly to the grid in Cases 2 and 3, hence the sold energy is lower than those in the other cases. Although the V2G and ESS-to-grid are not available, Cases 2 and 3 provide the acceptable level of PLR and TEC compared to Base Case and Case 1. Besides, Case 3 has the lowest battery degradation cost (710.21 ¢), followed by Case 2 (836.30 ¢). These results validate the effectiveness of the proposed ECM in the lack of bidirectional power flow for the shared ESS and EV fleet. Also, the proposed method procures a significant cost saving for the houses in the neighborhood as seen in Table 6. As a result, Case 5, which includes the shared ESS of 300 kWh, V2G/V2H services and ECM, is found as the most optimal case.

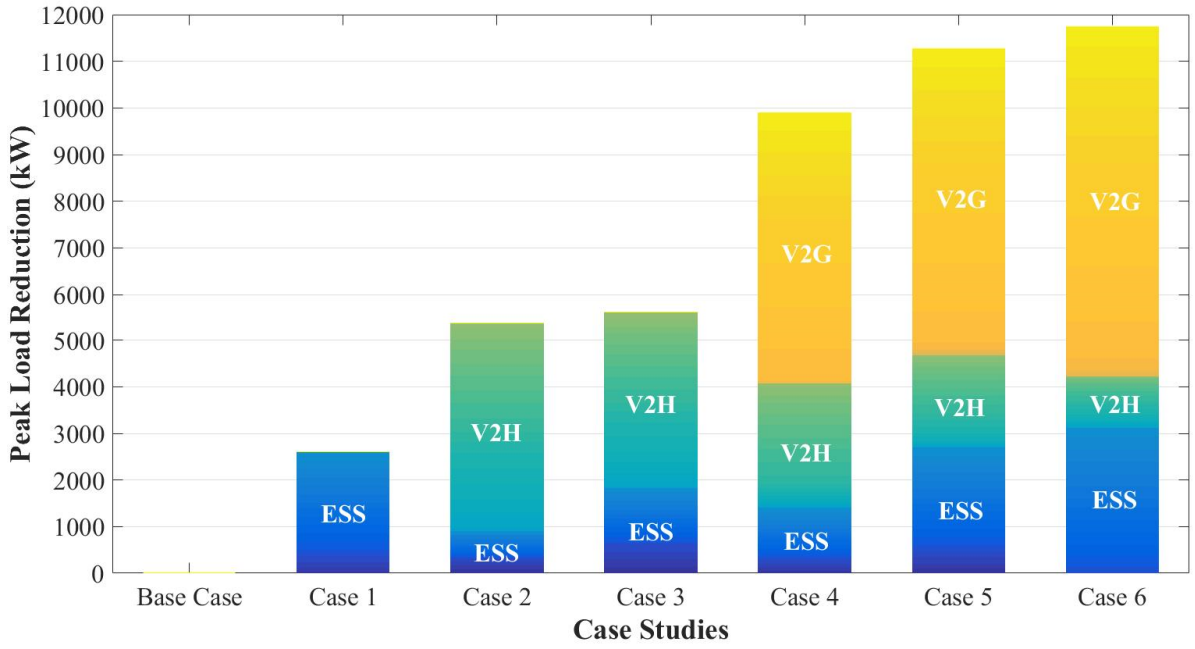

Figure 13. PLR values for each of cases during DR event.

Table 6. Comparison of the considered case studies

Case Studies	Purchased Energy [kWh]	Sold Energy [kWh]	PLR [MW]	Battery Degradation Cost [¢]	Total Energy Cost [¢]
Base Case	2648.11	--	--	--	17360.1
Case 1	2392.83	367.01	2.60	--	12434.5
Case 2	2453.11	352.73	5.39	836.30	11818.9
Case 3	2388.92	290.89	5.63	710.21	11652.9
Case 4	2938.47	863.75	9.89	1579.15	10238.6
Case 5	2913.27	868.16	11.26	1594.06	9734.9
Case 6	2942.50	857.91	11.74	1602.30	9473.9

4. Conclusions and Future Work

In this study, an energy management strategy including ECM and PLR-based DR program was implemented in a microgrid environment to reduce the energy cost of the end-users and decrease the peak load demand on the power grid. Energy credits gained by the end-users via excess renewable energy or via the current SoE level of their EV at the arrival time are used during the peak periods through the shared ESS or V2G/V2H services. Therefore, in consideration of the dynamic pricing tariff, both the houses and LSE obtain significant advantages by using these services. A set of case studies was tested to reveal the effectiveness of the proposed algorithm. The results obtained show that the proposed method reduces the TEC of the neighborhood by 43.9% and 21.7% for the Base Case and Case 1, respectively when compared to the cases without V2G/V2H services. Besides, it reduces the TEC by 17.6% and 16.5% for Case 2 and Case 3, respectively, when compared to the cases without V2G service. Furthermore, while the proposed case reduces the TEC by 4.92% when compared to Case 4, it only increases the TEC by 2.68% compared to Case 6. It should be indicated for the proposed case that the peak loading in the neighborhood area during the DR period decreases 78.7%, 62.1%, 32.9% and 25.8% in comparison with the Base Case, Cases 1, 4 and 6, respectively. Although the proposed case performs worse than Case 2 and 3 in reducing the peak loading in the neighborhood, it performs better in terms of the total PLR.

As a result of the conducted analyses, it can be concluded that the implementation of EVs with V2G and V2H technologies into a microgrid enables the economic and technical benefits for the LSE and end-users. It is clear that, in a case implementing multiple microgrids composed of numerous end-users with greater EVCS capacity, more substantial advantages can be achieved. As a future study, it is aimed to consider multiple microgrids including wind farms whose energy production generally coincides with EV charging period by integrating new constraints such as day-ahead and real-time market operations or a certain PLR level imposed by LSE.

Acknowledgement

The work of A. Taşcıkaraoğlu is supported by the Turkish Academy of Sciences (TUBA) within the framework of the Distinguished Young Scientist Award Program (GEBIP).

References

[1] J. Jannati and D. Nazarpour, "Optimal energy management of the smart parking lot under demand response program in the presence of the electrolyser and fuel cell as hydrogen storage system," *Energy Convers. Manag.*, vol. 138, pp. 659–669, 2017, doi: 10.1016/j.enconman.2017.02.030.

[2] "International Energy Agency (IEA)," 2021. www.iea.org/reports/global-ev-outlook-2021.

[3] A. Çiçek, A. K. Erenoğlu, O. Erdinç, A. Bozkurt, A. Taşcıkaraoğlu, and J. P. S. Catalão, "Implementing a demand side management strategy for harmonics mitigation in a smart home using real measurements of household appliances," *Int. J. Electr. Power Energy Syst.*, vol. 125, no. December 2019, 2021, doi: 10.1016/j.ijepes.2020.106528.

[4] S. Güner, A. K. Erenoğlu, İ. Şengör, O. Erdinç, and J. P. S. Catalão, "Effects of on-site pv generation and residential demand response on distribution system reliability," *Appl. Sci.*, vol. 10, no. 20, pp. 1–13, 2020, doi: 10.3390/app10207062.

[5] M. Song, M. Amelin, E. Shayesteh, and P. Hilber, "Impacts of flexible demand on the reliability of power systems," *2018 IEEE Power Energy Soc. Innov. Smart Grid Technol. Conf. ISGT 2018*, pp. 1–5, 2018, doi: 10.1109/ISGT.2018.8403357.

[6] M. F. Ribeiro, M. Shafie-Khah, G. J. Osório, N. Hajibandeh, and J. P. S. Catalão, "Optimal demand response scheme for power systems including renewable energy resources considering system reliability and air pollution," *Conf. Proc. - 2017 17th IEEE Int. Conf. Environ. Electr. Eng. 2017 1st IEEE Ind. Commer. Power Syst. Eur. EEEIC / I CPS Eur. 2017*, no. 309048, 2017, doi: 10.1109/EEEIC.2017.7977698.

[7] B. Yu, F. Sun, C. Chen, G. Fu, and L. Hu, "Power demand response in the context of smart home application," *Energy*, vol. 240, p. 122774, 2022, doi: 10.1016/j.energy.2021.122774.

[8] O. Erdinc, A. Tascikaraoglu, N. G. Paterakis, and J. P. S. Catalao, "Novel Incentive Mechanism for End-Users Enrolled in DLC-Based Demand Response Programs Within Stochastic Planning Context," *IEEE Trans. Ind. Electron.*, vol. 66, no. 2, pp. 1476–1487, 2019, doi: 10.1109/TIE.2018.2811403.

[9] I. Sengor, S. Guner, and O. Erdinc, "Real-Time Algorithm Based Intelligent EV Parking Lot Charging Management Strategy Providing PLL Type Demand Response Program," *IEEE Trans. Sustain. Energy*, vol. 12, no. 2, pp. 1256–1264, 2021, doi: 10.1109/TSTE.2020.3040818.

[10] I. Sengor, O. Erdinc, B. Yener, A. Tascikaraoglu, and J. P. S. Catalao, "Optimal energy management of EV parking lots under peak load reduction based DR programs considering uncertainty," *IEEE Trans. Sustain. Energy*, vol. 10, no. 3, pp. 1034–1043, 2019, doi: 10.1109/TSTE.2018.2859186.

[11] A. Walker and S. Kwon, "Design of structured control policy for shared energy storage in residential community: A stochastic optimization approach," *Appl. Energy*, vol. 298, no. February, p. 117182, 2021, doi: 10.1016/j.apenergy.2021.117182.

[12] J. P. Torreglosa, P. García-Triviño, L. M. Fernández-Ramirez, and F. Jurado, "Decentralized energy management strategy based on predictive controllers for a medium voltage direct current photovoltaic electric vehicle charging station," *Energy Convers. Manag.*, vol. 108, pp. 1–13, 2016, doi: 10.1016/j.enconman.2015.10.074.

[13] H. Chamandoust, S. Bahramara, and G. Derakhshan, "Day-ahead scheduling problem of smart micro-grid with high penetration of wind energy and demand side management strategies," *Sustain. Energy Technol. Assessments*, vol. 40, no. March, p. 100747, 2020, doi: 10.1016/j.seta.2020.100747.

[14] D. Prudhviraj, P. B. S. Kiran, and N. M. Pindoriya, "Stochastic Energy Management of Microgrid with Nodal Pricing," *J. Mod. Power Syst. Clean Energy*, vol. 8, no. 1, pp. 102–110, 2020, doi: 10.35833/MPCE.2018.000519.

[15] V. V. V. S. N. Murty and A. Kumar, "Optimal energy management and techno-economic analysis in microgrid with hybrid renewable energy sources," *J. Mod. Power Syst. Clean Energy*, vol. 8, no. 5, pp. 929–940, 2020, doi: 10.35833/MPCE.2020.000273.

[16] A. Taşcıkaraoğlu, "Economic and operational benefits of energy storage sharing for a neighborhood of prosumers in a dynamic pricing environment," *Sustain. Cities Soc.*, vol. 38, pp. 219–229, Apr. 2018, doi: 10.1016/j.scs.2018.01.002.

[17] M. Honarmand, A. Zakariazadeh, and S. Jadid, "Optimal scheduling of electric vehicles in an intelligent parking lot considering vehicle-to-grid concept and battery condition," *Energy*, vol. 65, pp. 572–579, 2014, doi: 10.1016/j.energy.2013.11.045.

[18] M. van der Kam and W. van Sark, "Smart charging of electric vehicles with photovoltaic power and vehicle-to-grid technology in a microgrid; a case study," *Appl. Energy*, vol. 152, pp. 20–30, 2015, doi: 10.1016/j.apenergy.2015.04.092.

[19] B. Bibak and H. Tekiner-Mogulkoc, "The parametric analysis of the electric vehicles and vehicle to grid system's role in flattening the power demand," *Sustain. Energy, Grids Networks*, vol. 30, p. 100605, 2022, doi: 10.1016/j.segan.2022.100605.

[20] D. Tiwari, M. A. A. Sheikh, J. Moyalan, M. Sawant, S. K. Solanki, and J. Solanki, "Vehicle-to-Grid Integration for Enhancement of Grid: A Distributed Resource Allocation Approach," *IEEE Access*, vol. 8, pp. 175948–175957, 2020, doi: 10.1109/ACCESS.2020.3025170.

[21] X. Liu, "Research on Flexibility Evaluation Method of Distribution System Based on Renewable Energy and Electric Vehicles," *IEEE Access*, vol. 8, pp. 109249–109265, 2020, doi: 10.1109/ACCESS.2020.3000685.

[22] W. Wu and B. Lin, "Benefits of electric vehicles integrating into power grid," *Energy*, vol. 224, p. 120108, 2021, doi: 10.1016/j.energy.2021.120108.

[23] A. O. David and I. Al-Anbagi, "EVs for frequency regulation: Cost benefit analysis in a smart grid environment," *IET Electr. Syst. Transp.*, vol. 7, no. 4, pp. 310–317, 2017, doi: 10.1049/iet-est.2017.0007.

[24] S. A. Amamra and J. Marco, "Vehicle-to-Grid Aggregator to Support Power Grid and Reduce Electric Vehicle Charging Cost," *IEEE Access*, vol. 7, pp. 178528–178538, 2019, doi: 10.1109/ACCESS.2019.2958664.

[25] G. Abdelaal, M. I. Gilany, M. Elshahed, H. M. Sharaf, and A. El'Gharably, "Integration of Electric Vehicles in Home Energy Management Considering Urgent Charging and Battery Degradation," *IEEE Access*, vol. 9, pp. 47713–47730, 2021, doi: 10.1109/ACCESS.2021.3068421.

[26] S. Huang, W. Liu, J. Zhang, C. Liu, H. Sun, and Q. Liao, "Vehicle-to-grid workplace discharging economics as a function of driving

distance and type of electric vehicle," *Sustain. Energy, Grids Networks*, vol. 2, p. 100779, 2022, doi: https://doi.org/10.1016/j.segan.2022.100779.

[27] H. Farzin, M. Fotuhi-Firuzabad, and M. Moeini-Aghtaie, "A Practical Scheme to Involve Degradation Cost of Lithium-Ion Batteries in Vehicle-to-Grid Applications," *IEEE Trans. Sustain. Energy*, vol. 7, no. 4, pp. 1730–1738, 2016, doi: 10.1109/TSTE.2016.2558500.

[28] X. Han *et al.*, "A review on the key issues of the lithium ion battery degradation among the whole life cycle," *eTransportation*, vol. 1, p. 100005, 2019, doi: 10.1016/j.etran.2019.100005.

[29] O. Kolawole and I. Al-Anbagi, "Electric vehicles battery wear cost optimization for frequency regulation support," *IEEE Access*, vol. 7, pp. 130388–130398, 2019, doi: 10.1109/ACCESS.2019.2930233.

[30] J. Grove, "Vehicle Licensing Statistics Vehicle Licensing Statistics : 2021," vol. 1, no. April, pp. 1–9, 2021.

[31] G. J. Chen, Y. H. Liu, S. C. Wang, Y. F. Luo, and Z. Z. Yang, "Searching for the optimal current pattern based on grey wolf optimizer and equivalent circuit model of Li-ion batteries," *J. Energy Storage*, vol. 33, no. September 2020, p. 101933, 2021, doi: 10.1016/j.est.2020.101933.